



The role of the surface on microglia function: implications for central nervous system tissue engineering

Liliana R. Pires^{1,2}, Daniela N. Rocha^{1,2}, Luigi Ambrosio⁴, Ana Paula Pêgo^{1,2,3}

1. INEB—Instituto de Engenharia Biomédica, Porto, Portugal

2. Faculdade de Engenharia, Universidade do Porto, Porto, Portugal

3. Instituto de Ciências Biomédicas Abel Salazar, Universidade do Porto, Porto, Portugal

4. Department of Chemical Sciences and Materials Technology, National Research Council of Italy, Rome, Italy

Author for correspondence: e-mail: apego@ineb.up.pt

Originally published in: *J R Soc Interface*. 2015 Feb 6; 12(103): 20141224. <http://dx.doi.org/10.1098/rsif.2014.1224>

ABSTRACT

In tissue engineering, it is well accepted that a scaffold surface has a decisive impact on cell behaviour. Here we focused on microglia—the resident immune cells of the central nervous system (CNS)—and on their response to poly(trimethylene carbonate-co-1-caprolactone) (P(TMC-CL)) fibrous and flat surfaces obtained by electrospinning and solvent cast, respectively. This study aims to provide cues for the design of instructive surfaces that can contribute to the challenging process of CNS regeneration. Cell morphology was evidently affected by the substrate, mirroring the surface main features. Cells cultured on flat substrates presented a round shape, while cells with elongated processes were observed on the electrospun fibres. A higher concentration of the pro-inflammatory cytokine tumour necrosis factor- α was detected in culture media from microglia on fibres. Still, astrogliosis is not exacerbated when astrocytes are cultured in the presence of microglia-conditioned media obtained from cultures in contact with either substrate. Furthermore, a significant percentage of microglia was found to participate in the process of myelin phagocytosis, with the formation of multinucleated giant cells being observed only on films. Altogether, the results presented suggest that microglia in contact with the tested substrates may contribute to the regeneration process, putting forward P(TMC-CL) substrates as supporting matrices for nerve regeneration.

Version: Postprint (identical content as published paper) This is a self-archived document from i3S – Instituto de Investigação e Inovação em Saúde in the University of Porto Open Repository For Open Access to more of our publications, please visit <http://repositorio-aberto.up.pt/>

INSTITUTO
DE INVESTIGAÇÃO
E INOVAÇÃO
EM SAÚDE
UNIVERSIDADE
DO PORTO

Rua Alfredo Allen, 208
4200-135 Porto
Portugal

+351 220 408 800

info@i3s.up.pt

www.i3s.up.pt

Keywords: electrospinning, microglia, scaffold surface, myelin, multinucleated giant cell, nerve tissue engineering

1. Introduction

Microglia, the resident immune cells of the central nervous system (CNS), play a key role in the maintenance of CNS homeostasis and in the management of tissue response to injury, although representing only approximately 10% of the total number of glial cells [1]. Microglia can secrete both pro-inflammatory cytokines that may lead to cell death, and anti-inflammatory molecules and neurotrophic factors that contribute to neuroprotection and regeneration [2]. Furthermore, in the context of an injury to the CNS, microglia are involved in the clearance of myelin debris that accumulates owing to Wallerian degeneration. This process is of paramount importance as the accumulation of debris has been associated with the inhibition of axonal regeneration [3]. Consequently, the diversity of microglia activities turn these cells into an interesting target for new therapies in the context of CNS regeneration [4].

It is now well established that topographic cues can have a considerable influence on cellular processes such as cell adhesion and differentiation (see [5,6] for a review). Under the scope of the development of scaffolds for CNS tissue engineering, neurons have been under the spotlight, so far. It has been shown that fibrous surfaces support axonal guidance and growth [7–9], as well as stem-cell differentiation into the neuronal lineage [10,11]. The number of studies investigating the influence of surface features on glial cells is increasing, yet focused on astrocytes, mainly due to astrocytes' key role in the formation of the glial scar in response to an injury to the CNS [12]. Astrocytes have been found to orientate their filamentous structure according to the features of the surface [13–16]. Moreover, although some authors did not find significant alterations in astrocyte activation when cells were seeded on a fibrous surface in comparison with cells cultured on flat solvent-cast films (assessed in terms of glial fibrillary acidic protein (GFAP) and vimentin protein expression) [14], others claimed that the contact of astrocytes with fibres is able to promote a decrease in GFAP expression [15] and an increase in glutamate uptake, contributing to neuroprotection in vivo [16]. Furthermore, by using micropatterned grooved scaffolds, mature astrocytes were found to revert into radial glia-like cells and consequently to a more pro-regenerative phenotype [17]. These studies highlight that by providing appropriate physical stimuli it is possible to bias the response of glial cells to injury.

Despite the important role ascribed to microglia, studies on microglia–material interaction are still in the infancy and have been focused on materials/structures for the design of implantable electrodes. The chemistry of the surface was found to influence the cytokine release profile of microglia depending on its hydrophobicity [18]. In what concerns surface topography, the effect of nanostructured silicone or poly(dimethylsiloxane) surfaces on microglia morphology, adhesion [19,20] or motility [19] was also investigated. More recently, it was demonstrated that microglia interact mechanically with silicone micropillars on a surface, and are affected by surface stiffness [21].

Foreseeing the design of a tissue engineering scaffold that could contribute to regeneration in the CNS, we explored the use of poly(trimethylene carbonate-co- ϵ -caprolactone) (P(TMC-CL)) to obtain matrices with different surface features. The preparation of fibres of this biodegradable polymer by electrospinning was previously reported [22], as were its remarkable properties in the context of tissue engineering for regeneration of the peripheral [23,24] and the central nervous system [25]. It is noteworthy that P(TMC-CL) has been shown to stimulate cortical neuron polarization and promote axonal elongation. Moreover, even in the presence of myelin, cortical neurons cultured on P(TMC-CL) films were found to extend more neurites, demonstrating the ability of P(TMC-CL) to tame myelin inhibition in a CNS lesion scenario [25]. Here we investigate the response of microglia to P(TMC-CL)

surfaces prepared either by electrospinning or by solvent cast in order to gather important clues towards the design of instructive scaffolds that can contribute to the challenging process of CNS regeneration.

2. Material and methods

2.1. Polymer synthesis and characterization

The statistical P(TMC-CL) copolymer was prepared by ring-opening polymerization and subsequently purified as previously described [23]. The chemical composition of the purified copolymer was assessed by ^1H nuclear magnetic resonance (NMR) and found to contain 11% mol of TMC, which was in accordance with the monomer ratio charged (10% mol TMC). The average number molecular weight and polydispersity index of the purified polymer were determined by size exclusion chromatography [22] and were found to be 8.2×10^4 and 1.61, respectively.

2.2. Substrate preparation

P(TMC-CL) fibres were prepared by electrospinning as previously described [22]. In brief, 10% (w/v) P(TMC-CL) solutions in dichloromethane (DCM; Merck, Germany) were dispensed at a controlled flow rate of 1 ml h^{-1} using a syringe pump (Ugo Basile, Italy). An electric field of 1 kV cm^{-1} was applied (Gamma High Voltage Research, Inc., FL, USA) between the spinneret (inner diameter 0.8 mm) and the flat collector ($15 \times 15 \text{ cm}$). Fibres were collected during 1–1.5 h onto 13 mm glass coverslips (Menzel-Glaser, Germany) distributed on top of aluminium foil.

P(TMC-CL) films were prepared by solvent casting as follows. A P(TMC-CL) solution in DCM (6% (w/v)) was cast onto a glass Petri dish. The solvent was left to evaporate overnight under a DCM-saturated atmosphere at room temperature (20–25°C).

After preparation, electrospun fibres and solvent-cast films were vacuum-dried for 24 h (vacuum oven; Raypa, Spain). Subsequently, 14 mm discs were punched out, packed under vacuum after an argon purge and sterilized by gamma irradiation (25 kGy, ^{60}Co source).

2.3. Surface characterization

P(TMC-CL) samples were sputter-coated with gold–palladium for 90 s (SPI Supplies, PA, USA). Afterwards, the P(TMC-CL) surfaces were observed by scanning electron microscopy (SEM) using a Quanta 400FEG microscope (FEI, The Netherlands). The fibre diameter was quantified from SEM micrographs using image analysis software (ImageJ, v. 1.39; NIH, MD, USA). The fibre mean diameter and fibre diameter distribution were calculated from at least 100 measurements from three independent samples.

2.4. Primary cell isolation and culture

Primary cultures of microglia and astrocytes were obtained from postnatal (1–2 days) Wistar rat pups based on previously described procedures [26,27]. Briefly, pups were decapitated, the meninges were carefully stripped off and cortices dissected. Subsequently, the tissue was enzymatically digested using a papain solution ($0.2 \text{ units ml}^{-1}$; Sigma-Aldrich Química, Portugal) for 30 min at 37°C. The tissue was further dissociated using a pipette and, subsequently, plated into tissue culture treated flasks (Thermo Fisher Scientific, Portugal). The mixed glial cultures were maintained for 8–10 days at 37°C in high-glucose Dulbecco's modified Eagle medium (DMEM) supplemented with 10% (v/v) of heat-inactivated

(56°C, 30 min) fetal bovine serum (FBS) and 1% (v/v) penicillin/streptomycin (P/S; 10 000 U ml⁻¹ penicillin, 10 000 µg ml⁻¹ streptomycin), all supplied by Gibco (Life Technologies S.A, Spain).

To obtain microglia, after culture confluence, the mixed glial cultures were shaken for 1 h using an orbital shaker (IKA, Germany) at 160 r.p.m. and 37°C. The supernatant enriched with microglia was collected and centrifuged (200g, 5 min). Microglial cell culture purity was quantified after immunolabelling using CD11b antibody (1 : 200; Abcam, Belgium) and found to be above 90% (see details in the electronic supplementary material) in accordance with previous reports that used a similar isolation technique [18,28]. A total of 6 × 10⁴ viable cells ml⁻¹ were seeded on P(TMC-CL) substrates secured at the bottom of a 24-well plate with a silicone o-ring (Epidor, Spain) and cultured in DMEM/F12 medium (Gibco) supplemented with 10% FBS and 1% P/S for 1 or 5 days. Glass coverslips were used as the experimental control.

After collecting microglia, mixed glial cultures were shaken for an additional 22 h to remove oligodendrocytes. The remaining cell layer, mainly composed of astrocytes, was maintained in culture in supplemented DMEM.

2.5. Cytoskeleton immunolabelling

To analyse cell morphology, cells were fixed with paraformaldehyde (4% (w/v), in phosphate-buffered saline; PBS) and immunostained for F-actin as follows. Cell external fluorescence was quenched using 50 mM NH₄Cl (Merck) for 10 min. After washing with PBS (three times, 5 min) cells were permeabilized with 0.1% (v/v) Triton X-100 (in PBS) for 5 min. Afterwards, cells were washed with PBS, incubated with 5% (w/v) bovine serum albumin (BSA; Merck) in PBS for 30 min and, thereafter, incubated with Alexa Fluor 488 phalloidin (1 : 40; Invitrogen, Life Technologies). Subsequently, cells were washed with PBS and stained with 4',6-diamidino-2-phenylindole (DAPI, 0.1 µg ml⁻¹ in PBS; Sigma-Aldrich). Samples were observed under an inverted fluorescence microscope (Axiovert 200; Zeiss, Germany) or confocal microscope (Leica Microsystems, Germany).

2.6. Microglia morphology analysis

Microglia morphology was analysed using the Fraclac plug-in for ImageJ. The box counting fractal dimension (DB) [29] as well as morphometrics based on the convex hull were calculated. Images of the cytoskeleton (F-actin) of individual cells (n = 50) were applied, after conversion to binary images and manually outlining the cell contour. The morphometric parameters calculated include area and circularity, and the results are presented in pixels.

2.7. Cytokine quantification

At the defined time point, cell culture supernatants from microglia seeded on different P(TMC-CL) substrates were collected and, after centrifugation (16 000g, 4°C, 10 min) to remove cell debris, stored at -20°C for posterior analysis. Cell culture media from cells activated with lipopolysaccharide (LPS, 100 ng ml⁻¹, 3 h; Sigma-Aldrich) was also analysed to serve as the positive control for microglia activation [30].

Tumour necrosis factor-α (TNFα; RayBiotech, GA, USA) and interleukin-6 (IL-6), interferon-γ (INFγ) and interleukin-10 (IL-10; all supplied by Biolegend, CA, USA) were quantified from microglia culture supernatants by enzyme-linked immunosorbent assay (ELISA) following the manufacturer's instructions.

2.8. Myelin phagocytosis assay

Myelin phagocytosis by microglia when seeded on different substrates was evaluated as follows. Rat brain myelin was obtained as previously described [31]. Five days after microglia seeding, a myelin suspension was added to the cell culture media to a final concentration of $2.5 \mu\text{g ml}^{-1}$ [32]. After 24 h in contact with myelin, cells were washed, stained for CD11b and subsequently fixed and permeabilized as described above. Cells were counterstained using myelin-binding protein (MBP) antibody (1 : 200; Chemicon, Millipore, MA, USA) at 4°C , overnight followed by 1 h of incubation with Alexa Fluor 488 donkey anti-rat IgG (1 : 1000; Invitrogen, Life Technologies). DAPI was applied to label cell nuclei. Cultures were observed using an inverted fluorescence microscope (Axiovert; Zeiss). Cells containing MBP (measure for myelin ingestion) and multinucleated giant cells (MGCs) were quantified from three different experiments and data are presented relative to the total number of cells.

2.9. Effect of microglia-conditioned media on astrocyte metabolic activity and gene expression

Astrocytes (4×10^4 viable cells ml^{-1} ; passage 4–7) were seeded on 24-well plates using supplemented DMEM. After adhesion overnight, the cell culture medium was changed to microglia-conditioned media collected after 5 days in contact with P(TMC-CL) substrates. As a control condition (non-treated cells), astrocyte cultures were conducted in supplemented DMEM/F12 (microglia culture medium; see §2.4).

Cell metabolic activity was assessed after 24 and 72 h by two different methods. Cellular ATP content was measured using Celltiter-Glo (Promega, WI, USA), following the manufacturer's instructions. To assess resazurin metabolization, cells were incubated (4 h, 37°C) with a resazurin (Sigma-Aldrich) solution (0.1 mg ml^{-1} , in PBS) and the fluorescence ($\lambda_{\text{ex}} = 530 \text{ nm}$, $\lambda_{\text{em}} = 590 \text{ nm}$) in the cell culture medium was measured (Synergy Mx; Biotek, Portugal).

Expression of genes related to astrogliosis, namely GFAP, collagen IV and vimentin, was assessed. Cell lysis and RNA purification were performed using Quick-RNA MiniPrep from Zymo Research (CA, USA), according to the manufacturer's instructions. Reverse transcription was done with SuperScript III (Invitrogen). Primer sequences are provided in the electronic supplementary material. Hypoxanthine-guanine phosphoribosyltransferase (Hprt) was applied as the reference gene. Polymerase chain reaction (PCR) was performed using HotStarTaq DNA polymerase (Qiagen, USA) for 34 cycles. Quantification of band intensity was done using ImageLab software, version 3.0 (Bio-Rad, Portugal).

To quantify GFAP expression at the protein level, the protein was assessed in astrocyte cultures by immunocytochemistry. In brief, astrocytes treated with microglia-conditioned media were fixed using paraformaldehyde and fluorescently labelled using the anti-GFAP antibody (rabbit anti-GFAP, 1 : 500; Dako), according to the procedure described in §2.4. Images were acquired applying constant fluorescence intensity. At least 25 images for each treatment from two independent experiments were quantified using ImageJ software.

2.10. Statistical analysis

Statistical analysis was performed using prism 5.0 software (GraphPad, CA, USA). A parametric t-test was applied to assess differences in cell morphology parameters and GFAP expression. Statistical differences between groups for cytokine concentration, astrogliosis markers and myelin phagocytosis were calculated by applying the non-parametric Mann–Whitney test. A p-value lower than 0.05 was considered statistically significant and is denoted by * or *** if $p < 0.001$.

3. Results

3.1. Substrate characterization

By using different processing techniques (electrospinning and solvent casting), distinctive P(TMC-CL) surfaces were obtained, as observed in the representative SEM micrographs presented in figure 1. Solvent-cast films show a spherulitic morphology (figure 1a,b) characteristic of a semicrystalline material [33]. The preparation of P(TMC-CL) fibres by electrospinning was previously optimized [22]. Under the conditions selected for the present study, the prepared electrospun membranes show a typical fibrous and randomly oriented structure (figure 1c,d). Bead defects are not observed. The mean fibre diameter was determined to be $1.09 \pm 0.1 \mu\text{m}$, being the fibre diameter distribution as depicted in figure 1e.

3.2. Effect of P(TMC-CL) surfaces on microglia

3.2.1. Microglia morphology

The morphology of microglia cells when seeded on different P(TMC-CL) surfaces was analysed after immunolabelling of F-actin. Cell cytoskeleton organization was found to be significantly affected by the surface features, as can be observed in figure 2. On P(TMC-CL) films, microglia present a round shape and long protrusions (figure 2a). Conversely, microglia seeded on P(TMC-CL) electrospun fibres show a smaller and more elongated cytoplasm (figure 2b), with actin concentrated at the points of cell adhesion along the fibre (figure 2b). Image analysis shows that microglia seeded on P(TMC-CL) films has an increased complexity compared with cells cultured on fibres, as indicated by the higher box counting fractal dimension DB [29]. Moreover, cell area was also found to be significantly increased on microglia seeded on P(TMC-CL) films (figure 2c). Although no statistical differences were found comparing mean values of circularity, it can be observed from the graphs representing the tercile distribution of the data (division of the distribution into three parts, each containing one-third of the population) that on P(TMC-CL) films a higher percentage of cells show a circularity close to 1—the theoretical circularity of a circle (figure 2d).

3.2.2. Cytokine release profile

Variations on microglia morphology have been traditionally associated with distinct functional states [34,35]. Therefore, to evaluate whether the differences found on microglia morphology, when seeded on the different P(TMC-CL) surfaces, can lead to alterations in cytokine release profile, IL-10 and TNF α were quantified in the cell culture medium at day 1 of culture and IL-10, TNF α , IL-6 and INF γ at day 5 of culture (figure 3). Although the differences did not achieve statistical significance, a higher concentration of the anti-inflammatory cytokine IL-10 was detected on the cell culture medium from microglia cultured on P(TMC-CL) fibres than on the medium obtained from cells seeded on solvent-cast films (figure 3a,b). Additionally, TNF α was found to be increased in the cell culture medium of cells adhered to the P(TMC-CL) fibrous surface, as compared with cells adhered on solvent-cast films; this difference was statistically significant at day 1 of culture (figure 3a). At day 5 of culture, the concentration of both TNF α and IL-6 tend to be increased, not statistically significant though (figure 3c). It is worthwhile mentioning that a sharp increase in TNF α and IL-6 concentration was observed when microglia were stimulated with LPS (figure 3c). The concentration of INF γ was found to be low and close to the detection limit of the ELISA performed (3.2 pg ml^{-1}), resulting in no differences between samples (data not shown).

Analysing the concentration of cytokines in the cell culture media over time, it can be observed that when cells were cultured in contact with P(TMC-CL) fibres the IL-10 concentration tended to increase, whereas the TNF α concentration was maintained. In the case of cells cultured on P(TMC-CL) films, no alteration in cytokine concentration was detected between the two time points analysed (figure 3).

3.2.3. Myelin phagocytosis

One of the key functions of microglia in the aftermath of a lesion to the CNS is the clearance of myelin debris since myelin accumulation exposes inhibitory molecules converting the lesion region into a non-permissive substrate for axonal regrowth [3]. To investigate whether the surface can influence the ability of microglia to phagocytose myelin, myelin was added in suspension to cells cultured on the different substrates and the percentage of cells engulfing myelin was quantified after immunolabelling.

The overall percentage of microglia found to engulf myelin was greater than 60% for cells cultured both on P(TMC-CL) films and on P(TMC-CL) fibres, with this parameter tending to be higher for cells seeded on films (figure 4a). As previously mentioned, cell morphology is markedly influenced by the P(TMC-CL) surface. Figure 4 shows that it is further affected by the presence of myelin. The round cells with long protrusions found on P(TMC-CL) films (figure 2) were able to form MGCs when in contact with myelin (figure 4b,c). On the other hand, in the microglia cultures performed in contact with fibrous substrates, MGCs were not observed (figure 4b). Conversely, cells tend to increase the number of ramifications (figure 4d).

3.3. Effect of microglia-conditioned media on primary astrocyte cultures

3.3.1. Astrocyte metabolic activity

The increase in astrocyte proliferation is one of the events associated with reactive astrogliosis, which is widely used as a pathological hallmark of the injured CNS [36]. Microglia cells are the immune regulators of astrogliosis [37], namely by releasing a variety of cytokines [36]. To understand whether microglia cells cultured on different (TMC-CL) surfaces can release factors with an impact on astrocytes, astrocyte metabolic activity was assessed after being cultured with microglia-conditioned media. Measures of metabolic activity were taken to be indicative of cell proliferation.

The cell metabolic activity of astrocytes when in contact with microglia-conditioned media showed a tendency to increase compared with the cell metabolic activity of non-treated cells (figure 5a,b). Conditioned media obtained from microglia cultures on P(TMC-CL) fibres or solvent-cast films were found to have a similar effect on astrocyte metabolic activity (figure 5a,b). Comparable results were obtained when astrocyte metabolic activity was assessed after 72 h in contact with microglia-conditioned media (data not shown). Figure 5c shows the typical morphology [38] of the astrocytic cell culture. No alterations were identified after incubating astrocytes with the different microglia-conditioned media under investigation.

3.3.2. Expression of astrogliosis markers

Astrogliosis has been associated with the upregulation of some genes, namely GFAP and vimentin [12]. Collagen type IV is the main constituent of the glial scar and its expression is increased in astrocytes in response to injury [39].

Astrocyte expression of astrogliosis gene markers was found not to be significantly affected by microglia-conditioned media in comparison with non-treated cells (figure 6a). Additionally, the P(TMC-CL) surface on which microglia were cultured did not show an effect on GFAP, vimentin or collagen type IV gene expression.

The expression of GFAP was assessed at the protein level by quantification of the fluorescence after GFAP immunolabelling. When using conditioned media from microglia cultured on P(TMC-CL) surfaces GFAP fluorescent labelling were decreased (figure 6b) compared with non-treated cells, suggesting that the factors released by microglia cultured on these surfaces do not activate astrocytes (figure 6b). Microglia-conditioned media obtained from cells seeded on glass coverslips was herein applied as an experimental control, leading to an increase in GFAP protein expression and confirming cell responsiveness in the experimental set-up applied (data not shown).

4. DISCUSSION

In the past few years, the understanding of the role of surface topographic features has gained substantial relevance in the context of the design of tissue engineering scaffolds for nerve regeneration. The focus was initially directed to neuronal cells [7,9,11] but more recent studies are contributing to shed some light on the effect of this parameter on other CNS cellular key players, such as astrocytes [14–17]. It is known that microglia, the immune cells of the CNS, play a critical role in CNS homeostasis as well as being in the frontline of the tissue response to injury [1]. Particularly, microglia cells can release cytokines and other molecules, activating cells at the lesion site, recruiting others and modulating their own function in an autocrine effect [37]. However, taking the role of microglia in a lesion scenario into consideration, the impact of the surface properties, in particular of topographical features, on the microglia response has been overlooked at large. This was the main goal of this study.

As previously reported for other cell types [6], in this work it was shown that microglia organize their cytoskeleton according to the features of the surface to which the cell adhere. On P(TMC-CL) solvent-cast films, microglia present a rounder shape and long protrusions, whereas on fibres the cell cytoskeleton elongates along the fibre direction and the cell area is smaller. Variations on microglia cell shape have been commonly taken as an indication of distinct functional states. Classically, amoeboid features have been associated with increased phagocytic and pro-inflammatory activities of microglia, whereas a ramified morphology suggests a quiescent state [34,35]. This classification is currently issue of active debate, as some reports show that different microglia activation states do not require alterations in cell morphology [40]. Still, the morphological features and functional state of microglia are correlated in different recent studies [41–43]. Here, the major differences in the morphology of microglia seeded on P(TMC-CL) substrates are reported. Although cell morphology was found to be neither marked amoeboid nor strictly ramified, it was observed that cells cultured on P(TMC-CL) films are larger (increased area) and tend to present an increased circularity. This cell shape could be considered an indication of a more pro-inflammatory profile. However, in regard to the cytokine release, it was found that microglia seeded on P(TMC-CL) films release less TNF α to the cell culture medium than cells adhered to fibres, at day 1 of culture. Extending the period of culture of microglia on the tested substrates resulted in no statistical differences in the release of both pro-inflammatory (IL-6 and TNF α) and anti-inflammatory (IL-10) cytokines. These results indicate that P(TMC-CL) surface features are determinant for microglia shape, but this does not impact long-term cytokine release, suggesting that cell shape is not a parameter on which one can directly predict functional state. A similar issue has been previously raised by Bartneck et al. [44] when comparing macrophages cultured on flat spin-coated films and hydrogel-coated nanofibres with variable fibre density (and pore size). The authors claimed that the effect on cell morphology and the expression of surface markers is

strongly affected by the biomaterial to which cells adhere. The analysis of microglia morphology using box counting analysis can bring new insights into this topic. The presented results show that cells seeded on P(TMC-CL) films have a higher complexity than cells cultured on fibres, as measured by the DB parameter. It has been proposed that microglia in the resting state have an increased complexity [29]. Taken together, our data suggest that microglia cultured on the P(TMC-CL) films are in a less activated state than cells cultured on fibres.

Interestingly, the effect of the surface features on cytokine release by primary microglia reported here shows a different trend compared to that described for macrophages. Previous studies using poly(L-lactide) [45] or poly(ϵ -caprolactone) [46] demonstrated that the concentration of pro-inflammatory molecules is lower in cultures in contact with electrospun fibrous surfaces than in cells on solvent-cast films. A surface topography that induces macrophage elongation was found to favour macrophage polarization into an anti-inflammatory phenotype, and, although the mechanisms are still not fully described, it was suggested that polarization via topographic signalling is mediated by actin cytoskeleton contractility [47]. The differences found in this study on microglia behaviour highlight the need for studying microglia in detail. Even though sharing relevant lineage features with macrophages, these cells can react differently to stimuli, as previously reported when testing different chemical factors [32,48].

In the context of an injury to the CNS, the contribution of microglia to the clearance of debris is of primary importance, as inefficient removal of myelin debris is associated with the inhibition of nerve regeneration [3]. It has been demonstrated that myelin phagocytosis is affected by the stimulation of microglia with different cytokines [32]. Thus, in the present work it was investigated whether culturing cells on different P(TMC-CL) surfaces can have an impact on microglia-mediated phagocytosis. A previous report showed that microglia in basal conditions or stimulated with anti-inflammatory cytokines (IL-4 and IL-13) were more efficient in myelin phagocytosis, with 70–75% of these cells being able to incorporate myelin in a phagocytosis assay. Conversely, less than 50% of the cells engulfed myelin if stimulated with LPS and INF γ [32]. In the context of Alzheimer's disease, it has been demonstrated that the accumulation of pro-inflammatory molecules such as LPS, IL-1 β or β -amyloid fibrils induces microglia dysfunction, limiting their phagocytic activity [49]. In this study, the percentage of cells that engulfed myelin was found to be above 60% for cultures conducted either on P(TMC-CL) solvent-cast films or on fibrous membranes. This result suggests that the P(TMC-CL) surfaces provide physical and/or chemical cues that promote phagocytosis without the need for additional chemical stimuli and may actively contribute to the establishment of a pro-regenerative environment.

Despite the fact that the percentage of cells that engulfed myelin was found not to be influenced by the surface, a remarkable difference was observed in microglia when in the presence of myelin. More than 10% of microglia seeded on P(TMC-CL) films were found to form MGCs, a phenomenon that was not observed when cells were adhered to fibres (0%). Although the morphology of microglia cells was affected by the surface features as described above, the formation of MGCs was clearly a consequence of the presence of myelin, as this event was not detected in its absence. The role of MGCs derived from microglia has been poorly discussed in the open literature. These cells have been found to accumulate with age [50], and are also associated with some neuropathologies, namely HIV-related dementia [51]. Microglia activation to form MGCs can be triggered by inflammatory cytokines [41,52,53] as well as in response to phagocytosis of cell debris [52,54]. MGCs have an increased phagocytic activity [52,54], which may represent an advantage when large amounts of debris accumulate due to Wallerian degeneration. To the best of our knowledge this is the first study that analyses the effect of the biomaterial surface on microglia in light of MGC formation. A recent publication using monocyte-derived macrophages demonstrates that orthogonal features on chitosan scaffolds favoured

macrophage fusion and MGC formation, comparing with a diagonal architecture [55]. Nonetheless, the authors were able to correlate this effect with the increase in TNF α in the cell culture media. In this study, the concentration of TNF α when cells were seeded on P(TMC-CL) films was found to be low, suggesting that this cytokine was not involved in the stimulation of MGC formation. It cannot be excluded that the concentration of TNF α was altered in the presence of myelin, but, if this was the case, it remains to be clarified why this was only in cells seeded on P(TMC-CL) films. In this context, the obtained results point out the importance of the substrate influencing directly the formation of MGCs. In our interpretation of the obtained results, the surface provided by electrospun fibres may be hampering cytoskeleton re-arrangement, cytoplasm enlargement and cell fusion, compromising, therefore, the formation of MGCs in comparison with what occurs on solvent-cast films.

There is increasing evidence that a reciprocal modulation between microglia and astrocytes takes place after CNS injury [56]. Microglia are the first cells arriving at the lesion site and the cytokines released by these cells, namely TNF α and IL-1 β , can induce astrocyte proliferation, influencing the glial scar formation [57]. On the other hand, molecules produced by astrocytes are believed to modulate microglia activation in the chronic phase of injury [56]. Taking these aspects into consideration, in this study it was investigated how the response of microglia to different surfaces can influence astrocyte activation markers. It was found that none of astrogliosis markers analysed are upregulated when astrocytes are treated with conditioned media from microglia cultured on P(TMC-CL) substrates. A previous study reported no activation of astrogliosis markers in astrocytes cultured with conditioned medium from resting microglia [58]. Therefore, our results point to the fact that the amount of pro-inflammatory cytokines produced by cells when seeded on P(TMC-CL) substrates does not trigger a significant activation of microglia that could, consequently, have an impact on astrocyte activation.

5. Conclusion

This work describes the effect of different substrates—P(TMC-CL) fibres and flat films—on primary microglia cells. Overall, the results presented show that both surfaces provide cues that may guide microglia towards a pro-regenerative profile, while evident differences were found on cell morphology, in line with the topographical features of the surface. Accordingly, it was pointed out that, when different surfaces are under investigation, microglia behaviour cannot be anticipated from cellular shape. Although the TNF α concentration was found to be increased in the early response to fibrous substrates, overall, the factors released by the cells were not able to trigger astrogliosis, independent of the surface. It is noteworthy that a significant percentage of microglia seeded on P(TMC-CL) substrates was found to participate in the phagocytosis of myelin. Moreover, only cells seeded on P(TMC-CL) flat films were able to form MGCs, pointing to the decisive role of the surface on the response of microglia to myelin debris. These results, along with our previous findings reporting that P(TMC-CL) has suitable properties for neuronal growth [24,25], put forward P(TMC-CL) as a supportive material for tissue regeneration in the context of an injury of the CNS.



Ethics statement

All experiments involving animals and their care were conducted in compliance with institutional ethics guidelines and with the approval of Portuguese Veterinary Authorities—Direcção-Geral de Alimentação e Veterinária (DGAV).

Acknowledgements

The authors acknowledge the Centro de Materiais da Universidade do Porto (CEMUP; REEQ/1062/CTM/2005 from FCT) for SEM and ¹H-NMR analyses. The authors wish to thank Renato Socodato for the fruitful discussions.

Funding statement

This work was financed by FEDER funds through the Programa Operacional Factores de Competitividade—COMPETE and by Portuguese funds through FCT—Fundação para a Ciência e a Tecnologia in the framework of the project PEst-C/SAU/LA0002/2011. L.P. and D.R. thank FCT for their PhD grants (SFRH/BD/46015/2008; and SFRH/BD/64079/2009).

REFERENCES

1. Aguzzi A, Barres BA, Bennett ML. 2013 Microglia: scapegoat, saboteur, or something else? *Science* 339, 156–161. (doi:10.1126/science.1227901)
2. David S, Kroner A. 2011 Repertoire of microglial and macrophage responses after spinal cord injury. *Nat. Rev. Neurosci.* 12, 388–399. (doi:10.1038/nrn3053)
3. Schwab JM, Bregtner K, Mueller CA, Failli V, Kaps HP, Tuli SK, Schluesener HJ. 2006 Experimental strategies to promote spinal cord regeneration—an integrative perspective. *Prog. Neurobiol.* 78, 91–116. (doi:10.1016/j.pneurobio.2005.12.004)
4. Hernandez-Ontiveros DG, Tajiri N, Acosta S, Giunta B, Tan J, Borlongan CV. 2013 Microglia activation as biomarker for traumatic brain injury. *Front. Neurol.* 26, 30. (doi:10.3389/fneur.2013.00030)
5. Curtis A, Wilkinson C. 1997 Topographical control of cells. *Biomaterials* 18, 1573–1583.
6. Martínez E, Engel E, Planell JA, Samitier J. 2009 Effects of artificial micro- and nano-structured surfaces on cell behaviour. *Ann. Anat.* 191, 126–135.
7. Liu T, Houle JD, Xu J, Chan BP, Chew SY. 2012 Nanofibrous collagen nerve conduits for spinal cord repair. *Tissue Eng. A* 18, 1057–1066. (doi:10.1089/ten.tea.2011.0430)
8. Nisbet DR, Rodda AE, Horne MK, Forsythe JS, Finkelstein DI. 2009 Neurite infiltration and cellular response to electrospun polycaprolactone scaffolds implanted into the brain. *Biomaterials* 30, 4573–4580. (doi:10.1016/j.biomaterials.2009.05.011)

Version: Postprint (identical content as published paper) This is a self-archived document from i3S – Instituto de Investigação e Inovação em Saúde in the University of Porto Open Repository For Open Access to more of our publications, please visit <http://repositorio-aberto.up.pt/>

INSTITUTO
DE INVESTIGAÇÃO
E INOVAÇÃO
EM SAÚDE
UNIVERSIDADE
DO PORTO

Rua Alfredo Allen, 208
4200-135 Porto
Portugal
+351 220 408 800
info@i3s.up.pt
www.i3s.up.pt

9. Yucel D, Kose GT, Hasirci V. 2010 Polyester based nerve guidance conduit design. *Biomaterials* 31, 1596–1603. (doi:10.1016/j.biomaterials.2009.11.013)
10. Xie J, Willerth SM, Li X, Macewan MR, Rader A, Sakiyama-Elbert SE, Xia Y. 2009 The differentiation of embryonic stem cells seeded on electrospun nanofibers into neural lineages. *Biomaterials* 30, 354–362. (doi:10.1016/j.biomaterials.2008.09.046)
11. Lim SH, Liu XY, Song H, Yarema KJ, Mao HQ. 2010 The effect of nanofiber-guided cell alignment on the preferential differentiation of neural stem cells. *Biomaterials* 31, 9031–9039. (doi:10.1016/j.biomaterials.2010.08.021)
12. Pekny M, Nilsson M. 2005 Astrocyte activation and reactive gliosis. *Glia* 50, 427–434. (doi:10.1002/glia.20207)
13. Chow WN, Simpson DG, Bigbee JW, Colello RJ. 2007 Evaluating neuronal and glial growth on electrospun polarized matrices: bridging the gap in percussive spinal cord injuries. *Neuron Glia Biol.* 3, 119–126. (doi:10.1017/S1740925X07000580)
14. Cao H, Marcy G, Goh ELK, Wang F, Wang J, Chew SY. 2012 The effects of nanofiber topography on astrocyte behavior and gene silencing efficiency. *Macromol. Biosci.* 12, 666–674. (doi:10.1002/mabi.201100436)
15. Min SK, Kim SH, Kim CR, Paik SM, Jung SM, Shin HS. 2013 Effect of topography of an electrospun nanofiber on modulation of activity of primary rat astrocytes. *Neurosci. Lett.* 534, 80–84. (doi:10.1016/j.neulet.2012.11.015)
16. Zuidema JM, Hyzinski-García MC, Van Vlasselaer K, Zaccor NW, Plopper GE, Mongin AA, Gilbert RJ. 2014 Enhanced GLT-1 mediated glutamate uptake and migration of primary astrocytes directed by fibronectin-coated electrospun poly-L-lactic acid fibers. *Biomaterials* 35, 1439–1449. (doi:10.1016/j.biomaterials.2013.10.079)
17. Mattotti M, Alvarez Z, Ortega JA, Planell JA, Engel E, Alcántara S. 2012 Inducing functional radial glia-like progenitors from cortical astrocyte cultures using micropatterned PMMA. *Biomaterials* 33, 1759–1770. (doi:10.1016/j.biomaterials.2011.10.086)
18. Leung BK, Biran R, Underwood CJ, Tresco PA. 2008 Characterization of microglial attachment and cytokine release on biomaterials of differing surface chemistry. *Biomaterials* 29, 3289–3297. (doi:10.1016/j.biomaterials.2008.03.045)
19. Amadio S, De Ninno A, Montilli C, Businaro L, Gerardino A, Volonté C. 2013 Plasticity of primary microglia on micropatterned geometries and spontaneous long-distance migration in microfluidic channels. *BMC Neurosci.* 14, 121. (doi:10.1186/1471-2202-14-121)
20. Persheyev S, Fan Y, Irving A, Rose MJ. 2011 BV-2 microglial cells sense micro-nanotextured silicon surface topology. *J. Biomed. Mater. Res. A* 99, 135–140. (doi:10.1002/jbm.a.33159)
21. Minev IR, Moshayedi P, Fawcett JW, Lacour SP. 2013 Interaction of glia with a compliant, microstructured silicone surface. *Acta Biomater.* 9, 6936–6942. (doi:10.1016/j.actbio.2013.02.048)
22. Pires LR, Guarino V, Oliveira MJ, Ribeiro CC, Barbosa MA, Ambrosio L, Pêgo AP. In press. Ibuprofen-loaded poly(trimethylene carbonate-co-1-caprolactone) electrospun fibers for nerve regeneration. *J. Tissue Eng. Regen. Med.* (doi:10.1002/term.1792)
23. Pêgo AP, Poot AA, Grijpma DW, Feijen J. 2001 Copolymers of trimethylene carbonate and epsilon-caprolactone for porous nerve guides: synthesis and properties. *J. Biomater. Sci. Polym. Ed.* 12, 35–53. (doi:10.1163/156856201744434)
24. Pêgo AP, Poot AA, Grijpma DW, Feijen J. 2003 Biodegradable elastomeric scaffolds for soft tissue engineering. *J. Control Release* 87, 69–79. (doi:10.1016/S0168-3659(02))
25. Rocha DN, Brites P, Fonseca C, Pêgo AP. 2014 Poly(trimethylene carbonate-co-1-caprolactone) promotes axonal growth. *PLoS ONE* 9, e88593. (doi:10.1371/journal.pone.0088593)

26. McCarthy K, de Vellis J. 1980 Preparation of separate astroglial and oligodendroglial cell cultures from rat cerebral tissue. *J. Cell Biol.* 85, 890–902.
27. Barateiro A, Miron VE, Santos SD, Relvas JB, Fernandes A, French-Constant C, Brites D. 2012 Unconjugated bilirubin restricts oligodendrocyte differentiation and axonal myelination. *Mol. Neurobiol.* 47, 632–644. (doi:10.1007/s12035-012-8364-8)
28. Cristóvão AC, Saavedra A, Fonseca CP, Campos F, Duarte EP, Baltazar G. 2010 Microglia of rat ventral midbrain recovers its resting state over time in vitro: let microglia rest before work. *J. Neurosci. Res.* 88, 552–562. (doi:10.1002/jnr.22219)
29. Karperien A, Ahammer H, Jelinek HF. 2013 Quantitating the subtleties of microglial morphology with fractal analysis. *Front. Cell. Neurosci.* 7, 1–34. (doi:10.3389/fncel.2013.00003)
30. Chang Y, Lee J, Hsieh C, Hsiao G, Chou D, Sheu J. 2009 Inhibitory effects of ketamine on lipopolysaccharide-induced microglial activation. *Mediators Inflamm.* 2009, 705379. (doi:10.1155/2009/705379)
31. Norton WT, Poduslo SE. 1973 Myelination in rat brain: method of myelin isolation. *J. Neurochem.* 21, 749–757.
32. Durafourt BA, Moore CS, Zammit DA, Johnson TA, Zaguia F, Guiot MC, Bar-Or A, Antel JP. 2012 Comparison of polarization properties of human adult microglia and blood-derived macrophages. *Glia* 60, 717–727. (doi:10.1002/glia.22298)
33. Pêgo AP, Vleggeert-Lankamp CLAM, Deenen M, Lakke EAJF, Grijpma DW, Poot AA, Marani E, Feijen J. 2003 Adhesion and growth of human Schwann cells on trimethylene carbonate (co)polymers. *J. Biomed. Mater. Res.* A67, 876–885. (doi:10.1002/jbm.a.10074)
34. Streit WJ, Walter SA, Pennell NA. 1999 Reactive microgliosis. *Prog. Neurobiol.* 57, 563–581. (doi:10.1016/s0304-0082(98)00069-0)
35. Shechter R, Schwartz M. 2013 Harnessing monocyte-derived macrophages to control central nervous system pathologies: no longer if 'but how'. *J. Pathol.* 229, 332–346. (doi:10.1002/path.4106)
36. Sofroniew MV, Vinters HV. 2010 Astrocytes: biology and pathology. *Acta Neuropathol.* 119, 7–35. (doi:10.1007/s00401-009-0619-8)
37. Zhang D, Hu X, Qian L, O'Callaghan JP, Hong JS. 2010 Astroglialosis in CNS pathologies: is there a role for microglia? *Mol. Neurobiol.* 41, 232–241. (doi:10.1007/s12035-010-8098-4)
38. Duarri A et al. 2011 Knockdown of MLC1 in primary astrocytes causes cell vacuolation: a MLC disease cell model. *Neurobiol. Dis.* 43, 228–238. (doi:10.1016/j.nbd.2011.03.015)
39. Liesi P, Kaupilla T. 2002 Induction of type IV collagen and other basement-membrane-associated proteins after spinal cord injury of the adult rat may participate in formation of the glial scar. *Exp. Neurol.* 173, 31–45. (doi:10.1006/exnr.2001.7800)
40. Boche D, Perry VH, Nicoll JAR. 2013 Review: activation patterns of microglia and their identification in the human brain. *Neuropathol. Appl. Neurobiol.* 39, 3–18. (doi:10.1111/nan.12011)
41. Lively S, Schlichter LC. 2013 The microglial activation state regulates migration and roles of matrix-dissolving enzymes for invasion. *J. Neuroinflamm.* 10, 75. (doi:10.1186/1742-2094-10-75)
42. Szabo M, Gulya K. 2013 Development of the microglial phenotype in culture. *Neuroscience* 241, 280–295. (doi:10.1016/j.neuroscience.2013.03.033)
43. Torres-Platas SG, Comeau S, Rachalski A, Bo GD, Cruceanu C, Turecki G, Giros B, Mechawar N. 2014 Morphometric characterization of microglial phenotypes in human cerebral cortex. *J. Neuroinflamm.* 11, 12. (doi:10.1186/1742-2094-11-12)

44. Bartneck M, Heffels KH, Pan Y, Bovi M, Zwadlo-Klarwasser G, Groll J. 2012 Inducing healing-like human primary macrophage phenotypes by 3D hydrogel coated nanofibres. *Biomaterials* 33, 4136–4146. (doi:10.1016/j.biomaterials.2012.02.050)
45. Saino E, Focarete ML, Gualandi C, Emanuele E, Cornaglia AI, Imbriani M, Visai L. 2011 Effect of electrospun fiber diameter and alignment on macrophage activation and secretion of proinflammatory cytokines and chemokines. *Biomacromolecules* 12, 1900–1911. (doi:10.1021/bm200248h)
46. Chen S, Jones JA, Xu Y, Low HY, Anderson JM, Leong KW. 2010 Characterization of topographical effects on macrophage behavior in a foreign body response model. *Biomaterials* 31, 3479–3491. (doi:10.1002/jbm.a.32609)
47. McWhorter FY, Wang T, Nguyen P, Chung T, Liu WF. 2013 Modulation of macrophage phenotype by cell shape. *Proc. Natl Acad. Sci. USA* 110, 17253–17258. (doi:10.1073/pnas.1308887110)
48. Lambert C, Ase AR, Séguéla P, Antel JP. 2010 Distinct migratory and cytokine responses of human microglia and macrophages to ATP. *Brain Behav. Immun.* 24, 1241–1248. (doi:10.1016/j.bbi.2010.02.010)
49. Pan XD, Zhu YG, Lin N, Zhang J, Ye QY, Huang HP, Chen XC. 2011 Microglial phagocytosis induced by fibrillar β -amyloid is attenuated by oligomeric β -amyloid: implications for Alzheimer's disease. *Mol. Neurodegener.* 6, 45. (doi:10.1186/1750-1326-6-45)
50. Hart AD, Wyttenbach A, Hugh Perry V, Teeling JL. 2012 Age related changes in microglial phenotype vary between CNS regions: grey versus white matter differences. *Brain Behav. Immun.* 26, 754–765. (doi:10.1016/j.bbi.2011.11.006)
51. Tambuyzer BR, Ponsaerts P, Nouwen EJ. 2009 Microglia: gatekeepers of central nervous system immunology. *J. Leukoc. Biol.* 85, 352–370. (doi:10.1189/jlb.0608385)
52. Hornik TC, Neniskyte U, Brown GC. 2014 Inflammation induces multinucleation of microglia via PKC inhibition of cytokinesis, generating highly phagocytic multinucleated giant cells. *J. Neurochem.* 128, 650–661. (doi:10.1111/jnc.12477)
53. Mosley K, Cuzner ML. 1996 Receptor-mediated phagocytosis of myelin by macrophages and microglia: effect of opsonization and receptor blocking agents. *Neurochem. Res.* 21, 481–487. (doi:10.1007/bf02527713)
54. Beyer M, Gimsa U, Eyuğoglu IY, Hailer NP, Nitsch R. 2000 Phagocytosis of neuronal or glial debris by microglial cells: upregulation of MHC class II expression and multinuclear giant cell formation in vitro. *Glia* 31, 262–266. (doi:10.1002/1098-1136(200009)31:3<262::aid-glia70.3.o.co;2-2)
55. Almeida CR, Serra T, Oliveira MI, Planell JA, Barbosa MA, Navarro M. 2014 Impact of 3-D printed PLA- and chitosan-based scaffolds on human monocyte/macrophage responses: unraveling the effect of 3-D structures on inflammation. *Acta Biomater.* 10, 613–622. (doi:10.1016/j.actbio.2013.10.035)
56. Gao Z, Zhu Q, Zhang Y, Zhao Y, Cai L, Shields CB, Cai J. 2013 Reciprocal modulation between microglia and astrocyte in reactive gliosis following the CNS injury. *Mol. Neurobiol.* 48, 690–701. (doi:10.1007/s12035-013-8460-4)
57. Buffo A, Rolando C, Ceruti S. 2010 Astrocytes in the damaged brain: molecular and cellular insights into their reactive response and healing potential. *Biochem. Pharmacol.* 79, 77–89. (doi:10.1016/j.bcp.2009.09.014)
58. Röhl C, Lucius R, Sievers J. 2007 The effect of activated microglia on astrogliosis parameters in astrocyte cultures. *Brain Res.* 1129, 43–52. (doi:10.1016/j.brainres.2006.10.057)

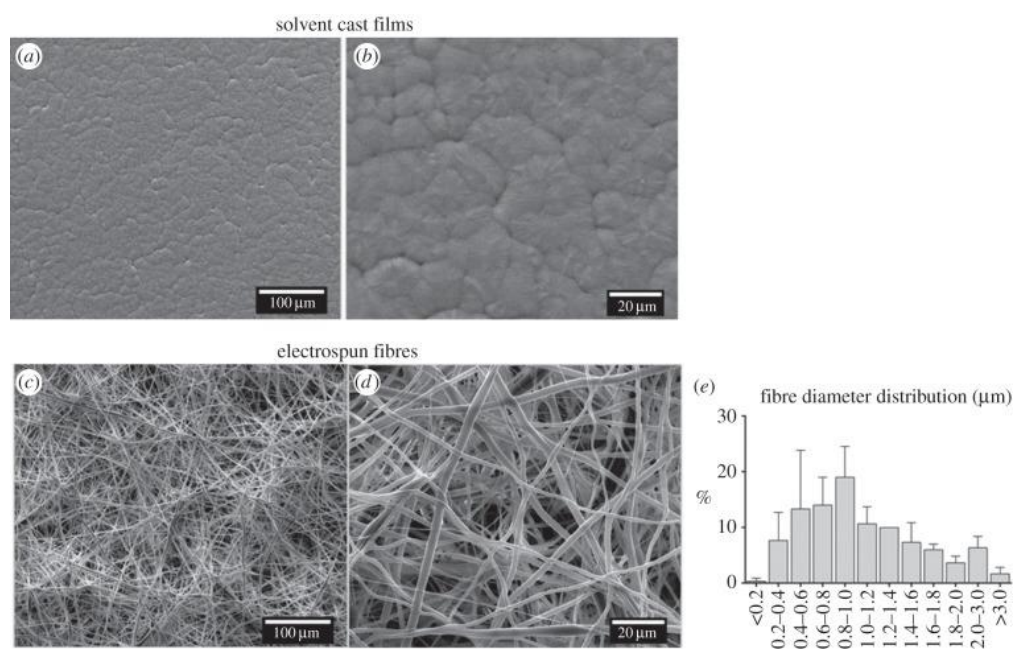


Figure 1. Scanning electron microscopy (SEM) photomicrographs of the prepared P(TMC-CL) surfaces. (a,b) Films obtained by solvent casting and (c,d) fibres obtained by electrospinning. (e) Fibre diameter distribution as calculated from 100 measurements from three independent samples (average \pm s.d.).

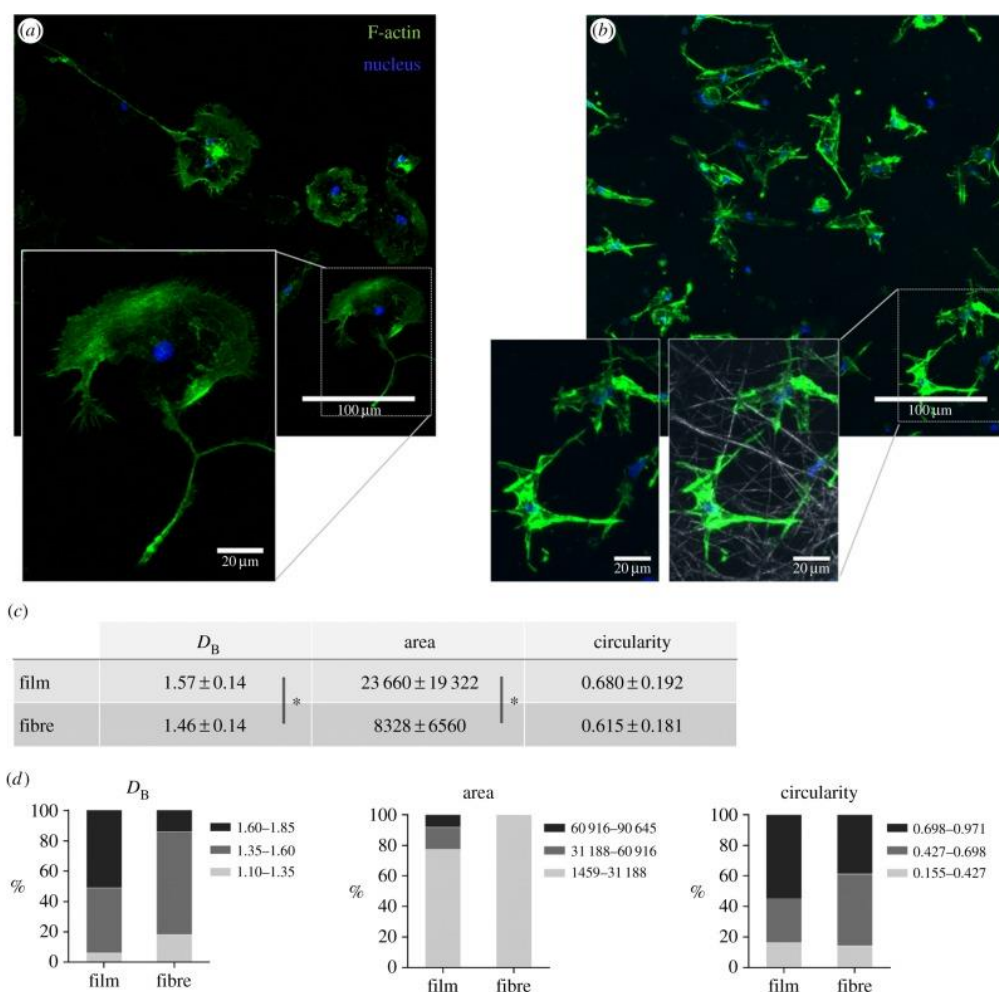


Figure 2. Microglia morphology when cultured (5 days) on P(TMC-CL) substrates. (a,b) Confocal Z-projection images of F-actin and cell nuclei of microglia seeded on P(TMC-CL) (a) films or (b) fibres. In the presented detail of (b) the fibrous structure of the electrospun mat (grey) is also shown. (c,d) Characterization of microglia morphology by image analysis using the box counting fractal dimension (D_B) and morphometrics based on a convex hull ($n = 50$). (c) Average \pm standard deviation values for the morphological parameters investigated: D_B , cell area and circularity. (d) Graphical representation of morphological parameters divided in terciles. Asterisks (*) denote statistical significance, $p < 0.05$.

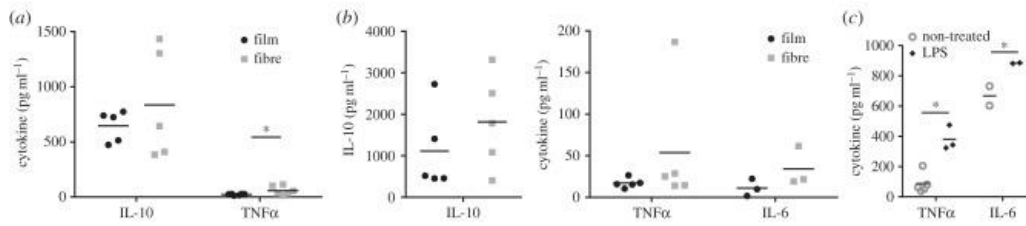


Figure 3. Cytokine release by microglia cultured on P(TMC-CL) substrates. Dot-plot showing the concentration of (a) IL-10 and TNF α in cell culture media after 1 or (b) 5 days in culture when seeded on P(TMC-CL) surfaces (n = 5). Panel (b) also shows the concentration of IL-6 (n = 3). (c) Release of pro-inflammatory cytokines (TNF α , IL-6) after microglia stimulation with lipopolysaccharide (100 ng ml⁻¹, 3 h, LPS). Asterisks (*) denote statistical significance, p < 0.05.

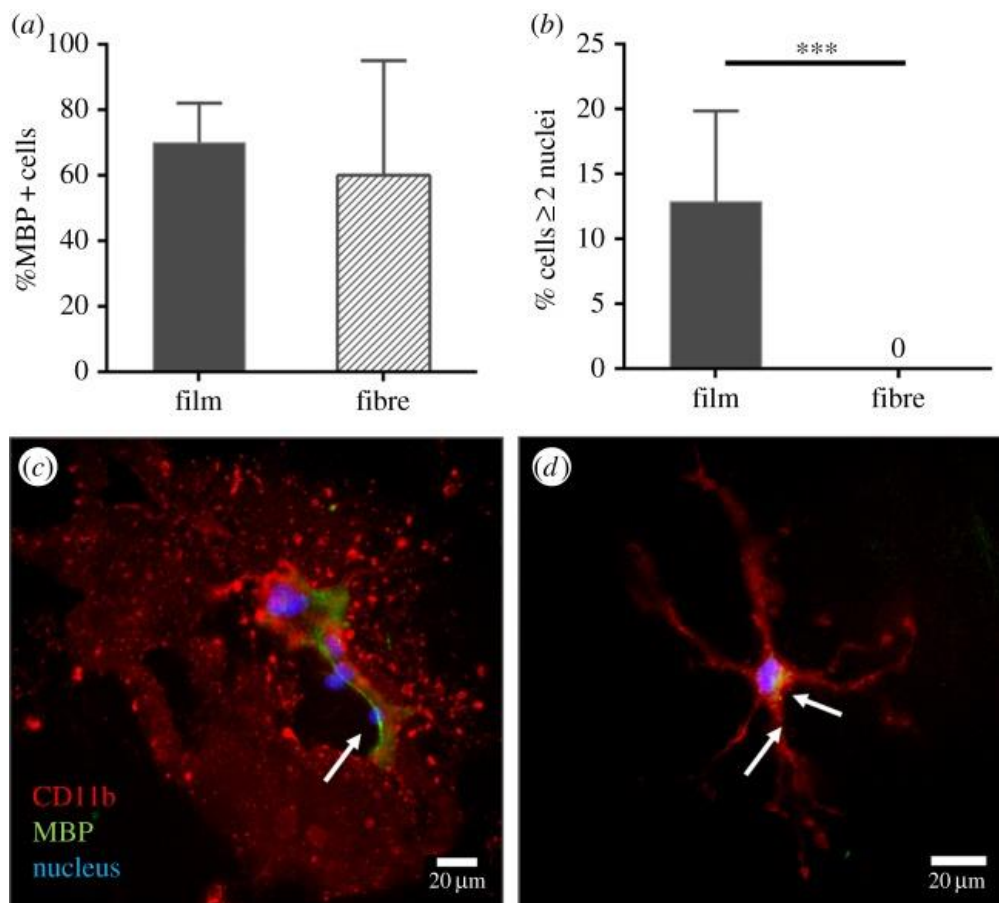


Figure 4. Myelin phagocytosis assay. (a) Quantification of the percentage of microglia cells that co-localize with myelin-binding protein (MBP). (b) Percentage of multinucleated giant cells found in microglia cultures seeded on P(TMC-CL) films, or fibres in the presence of myelin. Bars represent mean values and error bars show standard deviation (n = 3). Asterisks (***) denote statistical significance, p < 0.001. Version: Postprint (identical content as published paper) This is a self-archived document from i3s - Instituto de Investigação e Inovação em Saúde in the University of Porto Open Repository For Open Access to more of our publications, please visit <http://repositorio-aberto.up.pt/>

0.001. (c,d) Fluorescence microscopy images of microglia cultured on P(TMC-CL) (c) films and (d) fibres when in contact with myelin. Arrows indicate myelin inside the cells.

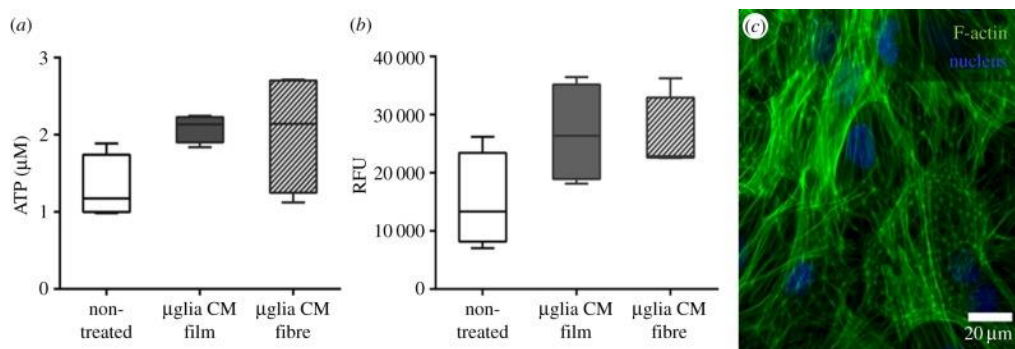


Figure 5. Astrocyte proliferation when in contact with microglia-conditioned media. Box-whisker plots ($n = 4$) showing (a) ATP production and (b) resazurin metabolism by astrocytes when in contact with microglia-conditioned media (μ glia CM) during 24 h. The medium was recovered from microglial cultures after 5 days in contact with P(TMC-CL) films or fibres. Non-treated cells were maintained in supplemented DMEM/F12 media. (c) F-actin labelling of astrocytes incubated with microglia-conditioned media obtained from cultures on fibrous meshes.

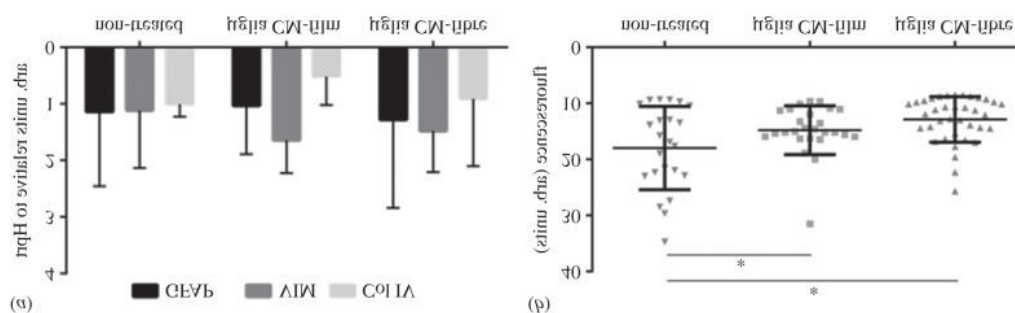


Figure 6. Expression of astroglial markers. (a) mRNA expression of glial fibrillary acidic protein (GFAP), vimentin (VIM) and collagen type IV (Col IV) in astrocytes treated with conditioned media obtained from microglia seeded on P(TMC-CL) solvent-cast films, or electrospun fibres, after 5 days in culture. Non-treated cells were maintained in supplemented DMEM/F12. Bars represent mean values and error bars show standard deviation ($n = 4$). (b) Fluorescence intensity of GFAP labelling in astrocytes cultured with microglia-conditioned media. Images were acquired with constant fluorescence intensity. At least 25 images were quantified from two independent experiments. Asterisks (*) denote statistical significance, $p < 0.05$.

Supplementary Materials

Microglial culture purity

The purity of microglial cultures was assessed by immunocytochemistry after labelling the conducted cultures with an antibody against CD11b (Abcam), following the manufacturer instructions. In brief, 24 hrs after seeding, cell culture medium was removed and the cells washed with phosphate buffered saline (PBS). The cells were incubated 20 minutes with CD11b antibody (diluted in DMEM, 1:200) at 37°C and, subsequently, with the secondary antibody (20 minutes, 1:500, anti-mouse AlexaFluor® 488, Invitrogen). Cells were then fixed using 4% (w/v) paraformaldehyde, permeabilized with Triton X-100 (0.2% (v/v) in PBS) and counterstained with 4',6-diamidino-2-phenylindole (DAPI, 0.1 µg.ml⁻¹ in PBS, Sigma). Cells were observed using an inverted fluorescence microscope (Axiovert, Zeiss) and the percentage of CD11b+ cells was calculated relative to the total number of cells (number of nuclei labelled with DAPI) and found to be above 90% (Figure 1, A).

Microglia cultures were also labelled for glial fibrillary acidic protein (GFAP) antibody in order to assess possible culture contamination with astrocytes. In brief, after fixation, cells were permeabilized 0.2% (v/v) Triton X-100 solution containing 5% (v/v) of normal goat serum (NGS, Sigma-Aldrich) during 30 minutes. Afterwards an anti-GFAP (Dako, 1:500) solution containing 1% (v/v) NGS and 0.15% (v/v) Triton X-100 was added and incubated overnight at 4°C. After washing with PBS (three times, 5 minutes), the cells were incubated with anti-rabbit AlexaFluor® 568 (Invitrogen) for 1 hr at room temperature. Cells were thereafter counterstained with DAPI as described above. The occurrence of GFAP positive cells was rare, consisting in less than 5% of the total number of cells (Figure 1, B).

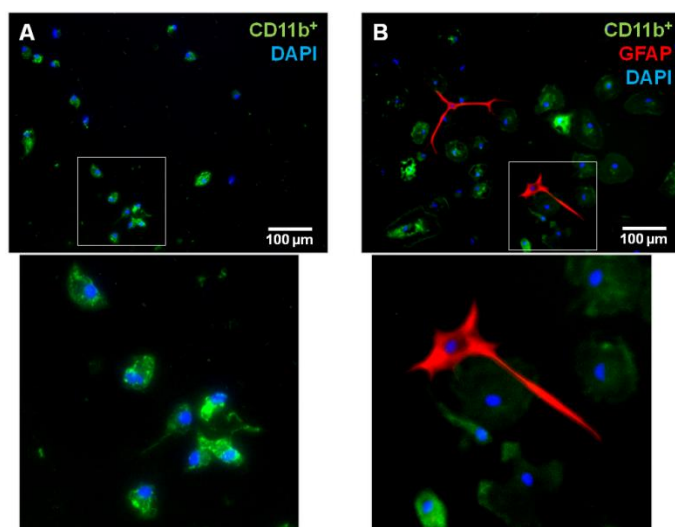


Figure 1. Microglia cultures immunolabelling. (A) CD11b⁺ cell detection or (B) combined with GFAP, an astrocytic marker.

Primer sequences applied in RT-PCR

Primer sequences used for RT-PCR were as follows:

GFAP sense	5'AGGCTGGAGGCGGAGAAC ₃ '
GFAP anti-sense	5'GCTGTGAGGTCTGGCTTGG ₃ '
Vimentin sense	5'CGTGATGTCCGCCAGCAGTATG ₃ '
Vimentin anti-sense	5'GGCATCCACTTCGCAGGTGAG ₃ '
Collagen IV sense	5'AAGGCGAGGAAGGCATCATG ₃ '
Collagen IV anti-sense	5'GGGTGAGTAGGCTGGAGGTC ₃ '
Hprt sense	5'ATGGACTGATTATGGACAGGACTG ₃ '
Hprt anti-sense	5'GCAGGTCAGCAAAGAACTTATAGC ₃ '